# 11. ZEOLITES IN SOUTH ATLANTIC DEEP-SEA SEDIMENTS

F. McCoy, Lamont-Doherty Geological Observatory, Palisades, New York
H. Zimmerman, Union College, Schenectady, New York
and
D. Krinsley, Queens College, C.U.N.Y., Flushing, New York and Arizona State University, Tempe, Arizona

## ABSTRACT

The stratigraphic and areal distribution of zeolites and their sedimentary associations in deep-sea sediments of the South Atlantic have been determined by examination of all available pre-Quaternary core and dredge material as well as sediment recovered from deep drilling. Clinoptilolite occurs in association with three dominant sediment components; volcanic, biosiliceous, and turbidite/clays, each of which may provide a source of silica for authigenic formation. Through time, the relative importance of these associations has changed significantly, reflecting the development of lithofacies and evolution of the South Atlantic basin.

## INTRODUCTION

Zeolites are known from many oceanic areas and occur in a variety of host sediments. They occur in surface sediments of the Pacific, Atlantic, and Indian oceans (Bonatti, 1963; Biscaye, 1965; Venkatarathnam and Biscaye, 1973), frequently over large areas, and have often been reported from older deep-sea sediments. The association of zeolites with areas of basic volcanism and their formation by the alteration of glassy volcanic material has been well documented (Bonatti, 1963; Hathaway and Sachs, 1965); yet occurrences are known where this association does not seem to be clear (Biscaye, 1965).

Phillipsite appears to be most common in Miocene and younger sediments of the Pacific and Indian oceans whereas clinoptilolite is more prevelant in Miocene and older sediments of the Atlantic Ocean (Bonatti, 1963; Biscaye, 1965; Venkatarathnam and Biscaye, 1973). This time relationship is, however, not understood in part due to the absence of systematic studies on the stratigraphic distribution of the zeolite minerals.

Leg 39 drilling in the South Atlantic (Figure 1) provided good recovery of older sediments. Because drilling sites rarely furnish an adequate regional coverage, additional samples were obtained from the Lamont-Doherty Geological Observatory (L-DGO) collection of cores and dredges in the South Atlantic Ocean. Using these materials, we have compiled a large data base for studying the distribution and occurrence of zeolites in South Atlantic deep-sea sediments.

## METHODS

Zeolites and their associated sedimentary components have been identified in samples from over 100 South Atlantic piston core and dredge samples in the L-DGO collection. All have been dated by Saito et al. (1974) and others as being pre-Quaternary (Table 1). Smear slides made from these samples were analyzed with a petrographic microscope. Visual estimates were made of the relative percentages of carbonate (subdivided in calcareous nannoplankton, foraminifers, and other carbonate material), biosiliceous material (not subdivided), terrigenous material (as sands and coarse silts, or clays), and other components, including zeolites. In most cases, zeolites were quite apparent under optical examination; even in low percentages, they were easily noted by their crystal shape and low refractive index. Roughly 40% of the smear slides were duplicated by McCoy and Zimmerman to ensure internal consistency in percentage estimates. In addition, carbonate was determined for all samples (methods given by McCoy and Zimmerman, this volume) to provide a quantitative control on visual estimates. Leg 39 samples were analyzed in an identical fashion. Data for previous DSDP cruises, Legs 3 and 14, were taken from the published Initial Reports volumes, and some preliminary data from Leg 36 has also been included.

Palinspastic base maps (Figures 6-12) for Cenozoic epochs and the Late and Early Cretaceous were made from the magnetic lineation chart of Pitman et al. (1974) with Africa held in its present position. (Geographic and physiographic areas mentioned here are identified in Figure 2.) These are not meant to be rigorous reconstructions, but are only intended to portray general relationships between continents and basins. (See McCoy and Zimmerman, this volume, for details on map construction.) All maps have the modern equivalent of the 2000 fathom (3660 m) contour line, shown only to suggest paleobathymetry. By consistently using modern continental outlines, marginal basins are ignored; an earlier (pre-Turonian) connection between the North and South Atlantic is not implied in the map of Early Cretaceous paleogeography. Subdivision of time slices by epochs

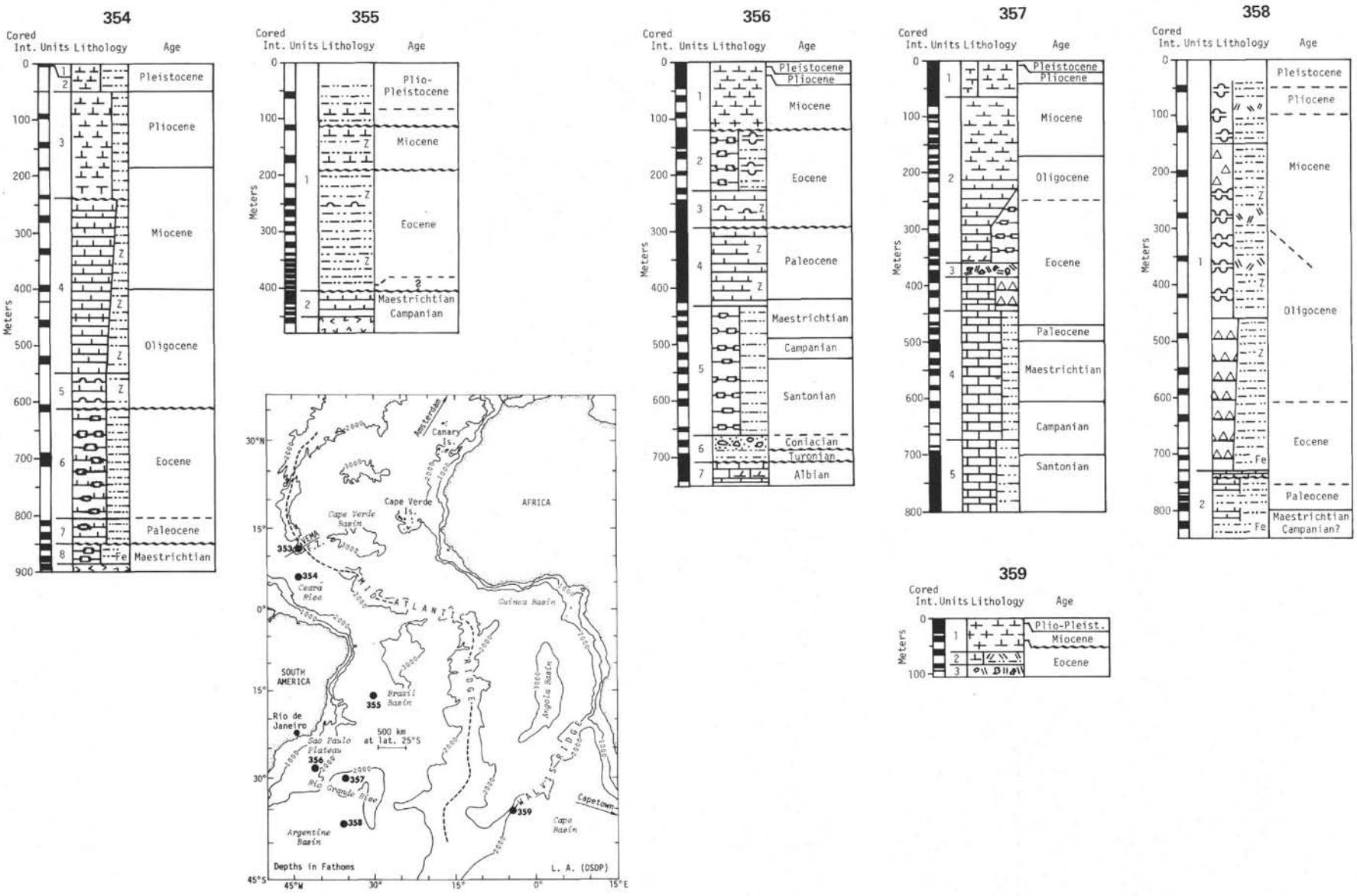


Figure 1. *Index chart of general stratigraphy at Leg 39 drilling sites and location of sites.*

TABLE 1
Piston Cores and Dredges Containing Zeolites[a]

| Core/Dredge Number | Latitude | Longitude | Water Depth (Corr.) m | Remarks |
|---|---|---|---|---|
| | | **Cretaceous** | | |
| V12-65 | 22°59'S | 08°07'E | 4118 | Maestrichtian |
| V17-144 | 40°34'S | 55°10'W | 2503 | Maestrichtian |
| V18-129 | 41°42'S | 56°35'W | 2039 | Maestrichtian; zeolites determined from XRD |
| V24-251 | 30°08'S | 39°28'W | 4111 | |
| V29-125 | 28°12'S | 02°45'E | 3129 | Maestrichtian-Campanian (?) zeolites determined from XRD |
| | | **Paleocene** | | |
| RC16-94 | 46°21'S | 59°32'W | 1028 | |
| V22-140 | 33°37'S | 02°21'E | 4433 | |
| V22-145 | 32°22'S | 02°09'E | 2056 | |
| V24-243 | 31°02'S | 35°43'W | 1020 | Determined from XRD |
| V26-81 | 23°46'S | 34°22'W | 4387 | |
| | | **Eocene** | | |
| E6-8 | 53°01'S | 55°48'W | 1992 | |
| RC8-2 | 11°12'N | 48°05'W | 4625 | |
| V18-RD29 | 55°29'S | 65°57'W | 1966-1719 | |
| V18-104 | 53°01'S | 52°52'W | 2880 | Determined from XRD |
| V18-130 | 41°30'S | 56°37'W | 1415 | Determined from XRD |
| V22-50 | 28°32'S | 29°00'W | 3566 | Determined from XRD |
| V22-51 | 28°32'S | 29°00'W | 933 | Determined from XRD |
| V22-149 | 31°26'S | 00°50'E | 4012 | Determined from XRD |
| V24-237 | 32°12'S | 26°44'W | 4193 | |
| V29-117 | 33°11'S | 02°58'W | 1730 | |
| V31-101 | 24°47'S | 42°02'W | 2321 | |
| V31-107 | 24°49'S | 42°03'W | 2294 | |
| | | **Oligocene** | | |
| RC12-296 | 37°04'S | 07°12'W | 2681 | |
| RC12-297 | 36°09'S | 06°43'W | 3528 | |
| | | **Miocene** | | |
| A180-99 | 16°14' | 35°21'W | 4206 | |
| E 9-3 | 50°36'S | 43°43'W | 2357 | |
| RC11-27 | 28°31'S | 30°04'W | 2704 | |
| RC11-88 | 41°11'S | 20°08'E | 5125 | |
| RC13-270 | 55°29'S | 04°38'E | 3160 | |
| V9-18 | 08°59'S | 15°55'W | 4005 | |
| V15-96 | 53°16'S | 68°10'W | 11 | Determined from XRD |
| V15-136 | 52°11'S | 49°05'W | 2514 | |
| V18-106 | 53°27'S | 50°24'W | 2638 | |
| V18-109 | 52°12'S | 45°42'W | 3232 | |
| V18-115 | 49°26'S | 50°42'W | 3493 | |
| V18-116 | 49°26'S | 50°28'W | 2367 | |
| V18-117 | 49°30'S | 52°15'W | 2559 | |
| V18-118 | 49°05'S | 52°43'W | 5319 | |
| V18-121 | 47°37'S | 55°29'W | 5236 | |
| V22-172 | 12°40'S | 09°49'W | 4127 | Determined from XRD |
| V22-181 | 02°21'S | 16°54'W | 4012-4438 | |
| V22-190 | 06°02'N | 21°16'W | 3491 | Determined from XRD |
| V22-RD10 | 16°03'S | 05°50'W | 2310-2096 | |
| V25-54 | 01°25'S | 37°23'W | 3056 | |
| V29-120 | 29°50'S | 02°38'E | 1805 | |
| V31-101 | 24°47'S | 42°02'W | 2321 | Determined from XRD |
| V31-112 | 25°07'S | 41°50'W | 2573 | Determined from XRD |

TABLE 1 – *Continued*

| Core/Dredge Number | Latitude | Longitude | Water Depth (Corr.) m | Remarks |
|---|---|---|---|---|
| | | **Pliocene** | | |
| A180-107 | 19°39'S | 36°04'S | 4023 | |
| C99-22 | 08°43'S | 06°43'S | 4660 | |
| E6-6 | 57°10'S | 58°50'W | 3710 | |
| E6-11 | 55°44'S | 56°03'W | 3980 | |
| E7-3 | 55°03'S | 44°40'W | 3553 | |
| RC8-15 | 19°21'S | 20°32'W | 4707 | |
| RC13-268 | 57°02'S | 00°06'W | 4005 | |
| V19-302 | 10°15'N | 25°22'W | 5583 | |
| V22-152 | 31°37'S | 00°58'E | 4319 | |
| V22-184 | 00°21'N | 17°31'W | 1712 | |
| V22-189 | 04°56'N | 21°07'W | 2525 | Determined from XRD |
| V25-73 | 08°39'N | 53°09'W | 4133 | |
| V31-107 | 24°49'S | 42°03'W | 2294 | Determined from XRD |

[a]Determinations of zeolites made from optical analyses of smear slides unless otherwise indicated; ship abbreviations as follows: A = Atlantis, C = Chain, E = Eltanin, RC = R. Conrad, V = Vema.

represents a convenience since much of the material available for study has been dated only to this degree. The Early Cretaceous time slice represents all samples of Albian age or older; Late Cretaceous are those of post Albian age.

DSDP drilling results, Leg 39 in particular, provide the vertical stratigraphic control for this work. These data show the variation in abundance of zeolites through time, as well as their association with general sediment types and other sedimentary components. Piston cores and dredges, however, only give an indication of horizontal variability within the basin for each time-slice; they do not represent the complete sequence for any epoch, but are a single point in an often long time sequence.

Samples of Leg 39 material were selected for X-ray diffraction analysis where relatively high percentages of zeolites were determined by on-board optical examination (Table 2). Secondarily, zeolites were also noted in the fine-grained fraction of samples chosen from each drill site and from a variety of sedimentological facies and stratigraphic horizons for clay mineral analysis (Zimmerman, this volume). Additionally, all piston core and dredge samples were subjected to X-ray diffraction (XRD) analysis.

Procedures of sample preparation are described in Jackson (1969) and Biscaye (1965). Calcium carbonate was dissolved by treatment with acetic acid solution and amorphous iron was dissolved by the method of Mehra and Jackson (1960). Preferred-orientation slides were prepared for the clay-sized materials (<4 $\mu$m), with analysis before and after glycolation. Coarser materials were separated by repeated decantation on the fine slurry after settling, a process that resulted in the concentration of the silt-sized (<16 $\mu$m) zeolite crystals when they were present. This material was then mounted on glass slides for analysis; powder-camera mounts were also prepared for the samples particularly rich in zeolite content (Table 3). In order to ascertain the presence of heulandite/clinoptilolite, the samples were also subjected to a sequential heating procedure (up to 600° for one hour; Mumpton, 1960: Hathaway and Sacks, 1965).

Slides were analyzed on a General Electric XRD-7 diffractometer with nickel filtered; Cu K$\alpha$ radiation at 2° 2$\phi$/min scanning speed. Semiquantitative estimates of the crystalline components were determined by concentration factors described by Rex (1969) and Zemmels and Cook (1973). These estimates are reported here on a ranked, semiquantitative scale (Table 2).

Selected samples were examined by Scanning Electron Microscopy (SEM). Primarily, these were from the Eocene section of Site 355 where quartz-rich sands of turbidite origin contain unusually high amounts (up to 30%) of zeolites (see Site 355, this volume). Samples were weighed dry, washed over a 44-$\mu$m sieve, and the dry residue weighed after being allowed to reach room temperature; the residue was then treated with 15% HCl to digest the calcium carbonate component. Zeolites and clay minerals may have also been attacked to some degree. After drying, the coarser quartz components were hand-picked under the binocular microscope and mounted on SEM stubs. Spot samples were examined with the polarizing microscope to make certain that quartz was not confused with sanidine or volcanic glass (Margolis, 1975). Samples were then coated with a layer of Pt-Pd metal, examined, and photographed with the scanning electron microscope. The number of grains available varied considerably from one sample to another. Generally, all grains were used if the sample contained less than 20 grains; for those samples containing more than this amount, only 20 were examined and photographed. Our experience indicates that this number of grains usually provides as much information as a population three times this amount.

## RESULTS

Zeolites are an authigenic component of deep-sea sediments frequently derived through the alteration of basic volcanic glass. The two most common minerals,

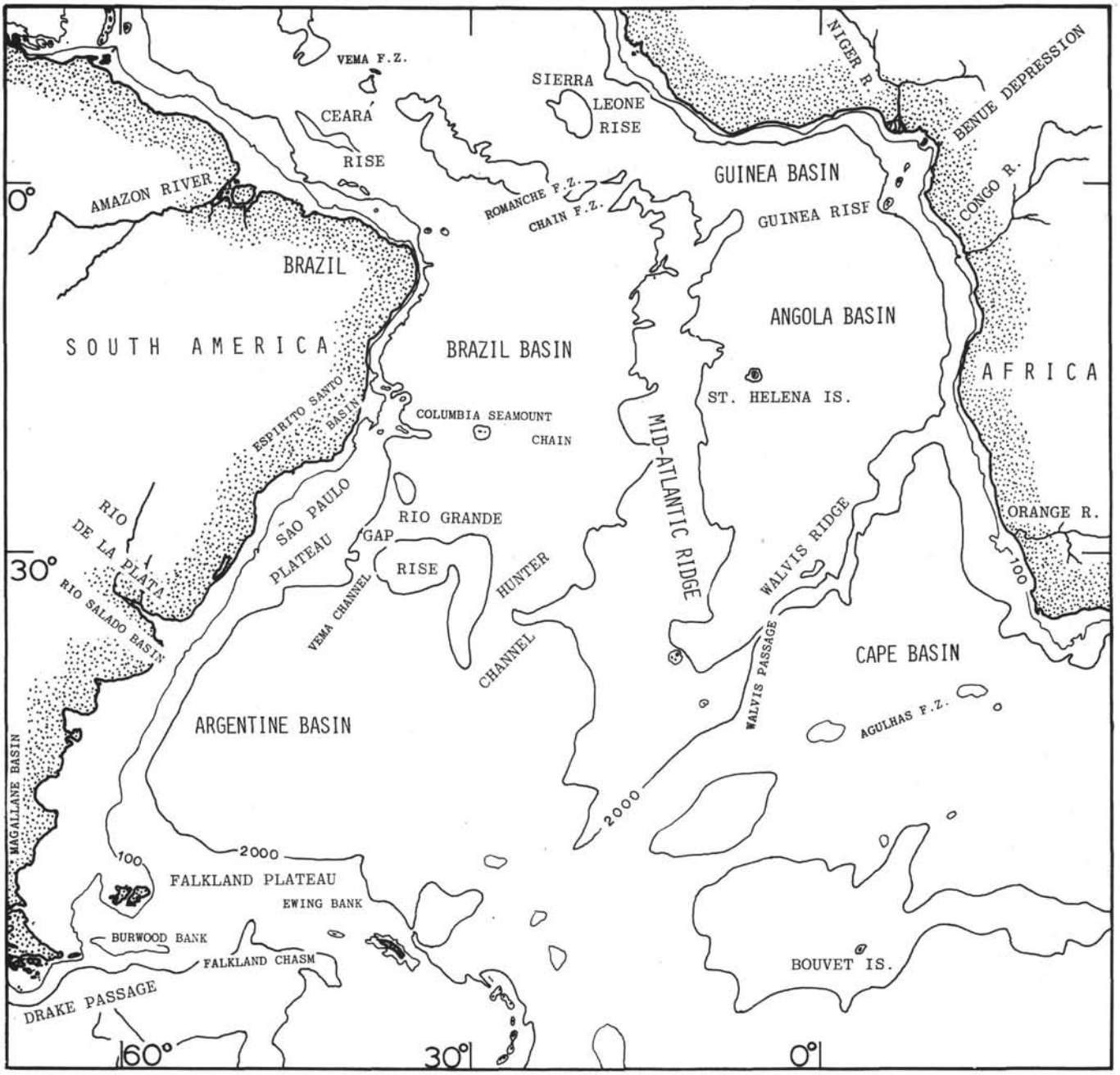


Figure 2. *Index chart of physiographic and geographic locations mentioned in text.*

phillipsite and clinoptilolite, are K and Na enriched zeolites. Heulandite, a zeolite less siliceous than clinoptilolite and relatively enriched in $Ca^{++}$, may also be present, but occurs in considerably lesser quantities. For the appropriately high Si/Al ratios, silica can be derived from the dissolution of siliceous fossils, the alteration of volcanics, diagenesis of plagioclase feldspars, or possibly through degradation of clays.

**Occurrence of Zeolites at Leg 39 Sites**

Zeolites occur at all Leg 39 Sites (Table 2) and are most common in the Brazil Basin (Site 355). A strong association with turbidite sequences is evident particularly in the Eocene, where basal, quartz-rich sand and silt layers contain up to 30% or more zeolites (visual smear-slide estimates). Following the deposition of Cretaceous limestones, this site passed beneath the CCD level and the turbidites represent deposition within an actively subsiding basin where carbonates were dissolved (Site 355, this volume; McCoy and Zimmerman, this volume; Boersma, this volume).

At all other sites, zeolites are present in substantially smaller amounts. On the Ceará Rise (354), they are common in the Oligocene and Miocene in association with siliceous fossils (5%-40% diatoms and Radiolaria, minor quantities of sponge spicules). Siliceous fossils, as well as amorphous masses of silica, also occur with zeolites in siliceous and marly chalks of Site 356 on the

TABLE 2
Results of X-ray Diffraction Analysis

| Sample (Interval in cm) | Silt-sized Fraction | | | | | | | | Clay-size Fraction | | | | | |
|---|---|---|---|---|---|---|---|---|---|---|---|---|---|---|
| | Clin. | Feld. | Qtz. | Mica | Kaol | Phil. | Barite | Cristo. | Clin. | Mont. | Ill. | Kaol | Age | Lithology |
| **Site 354** | | | | | | | | | | | | | | |
| 10, CC | Dom. | Tr | – | Tr | – | – | – | – | Tr | Dom | Tr | A | Oligocene | Zeolitic coccolith ooze |
| 11-2, 99 | A-Dom. | Tr | – | Tr | – | – | – | – | Tr-C | Dom | C | A | Oligocene | Zeolitic coccolith ooze |
| **Site 355** | | | | | | | | | | | | | | |
| 3-3, 118 | C | C | C | C | Tr | – | – | – | C | Dom | C | C-Tr | Oligocene | Zeolitic clay |
| 4-3, 121 | C-Tr | C-A | A | A | Tr | – | – | – | Tr | A-D0m | C | C | Eocene | Zeolitic clay |
| 5-6, 104 | C | Tr | Tr-C | Tr | – | Tr | Tr | – | Tr | Dom | Tr | Tr | Eocene | Dolomitic silty clay |
| 6-4, 6 | C | C | A | A | Tr | – | – | – | Tr | Dom | C | C | Eocene | Dolomitic silty clay |
| 6-5. 32 | C | C | A | – | – | – | – | – | C | Dom | Tr | Tr | Eocene | Dolomitic silty clay |
| 7-3, 99 | C | C | Tr | C | Tr | – | Tr-C | – | C-Tr | Dom | C | C | Eocene | Zeolitic clay |
| 11-4, 67 | C-Tr | – | C | Tr | – | – | – | C | – | A | A | C | Eocene | Zeolitic clay |
| 16-2, 122 | – | A | A-Dom | A-Dom | C | – | – | – | – | A | C-A-C | C | Paleocene | Silty clay |
| **Site 356** | | | | | | | | | | | | | | |
| 11-2, 32 | C | Tr | C | – | – | – | – | C | – | Dom | Tr | – | Eocene | Zeolitic carbonate clay |
| 17-3, 18 | Tr | C | C | C | – | – | – | C | Tr | Dom | C | – | Paleocene | Carbonate silty clay |
| 23-3, 71 | C | C | C | C | – | – | – | – | C | Dom | A | – | Paleocene | Carbonate silty clay |
| **Site 357** | | | | | | | | | | | | | | |
| 22-2, 83 | Dom. | ? | – | – | – | – | – | – | C | – | – | – | Eocene | Zeolitic carbonate ooze |
| 43-3, 99 | Tr | C | A | Tr | – | – | – | A-Dom | – | Tr | C | – | Santonean | Siliceous carbonate ooze |
| **Site 358** | | | | | | | | | | | | | | |
| 3-5, 136 | Tr | C | A | Tr | – | – | – | Tr | Tr | A | A | Tr | Miocene | Silty clay |
| **Site 359** | | | | | | | | | | | | | | |
| 4-1, 138 | – | C | – | Tr | Tr | – | – | Tr | – | Dom | – | – | Eocene | Silty carbonate clay |

Note: Quantity: Dom = Dominant, > 40%; A = Abundant; 25-40%; C = Common, 10-25%; Tr = Trace, <10%.

São Paulo Plateau, especially in the Paleocene and Eocene, but also in the Miocene and Pliocene. These occurrences are devoid of volcanic glass. Generally, other occurrences of zeolites are associated with small quantities of volcanic glass: in Cretaceous sections of Sites 356, 357, and 358; Paleocene at Sites 355 and 358, and in one small interval of Site 356; Eocene of Sites 357 and 359, and in a small portion of Site 358; and in the Miocene of Sites 356, 356A, and 358.

Zeolites are often associated with iron oxides, as well as, in decreasing amounts, authigenic dolomite, glauconite, fish teeth, and very rarely, authigenic feldspar and barite. It is difficult to see any pattern in these. Resorption of zeolites was occasionally noticed but has not yet been systematically studied for its geochemical implications or sedimentary associations.

## Mineralogy

Optical examination of silt-sized concentrates reveals separate, more or less euhedral crystals occasionally exhibiting a doubly terminating habit. This is especially prevalent in the samples from the Ceará Rise (Site 354, Figure 3). The zeolites at other sites are predominantly smaller, anhedral laths showing severe corrosion (some examples of corrosion may also be noted in Figure 3).

Clinoptilolite, the silica-rich zeolite of heulandite structure (Hay, 1966) was found with regularity on Leg 39. On the basis of the resistance of its structure to thermal attack the identification of clinoptilolite, rather than heulandite, was assured for most of the zeolite occurrences. The samples from the Ceará and Rio Grande rises, however, showed characteristics intermediate between clinoptilolite and heulandite under a sequential heating procedure; a comparison with X-ray powder data (Deer et al., 1963, Table 3) also suggests intermediate characteristics. Rather than the coexistence of both minerals, this behavior may indicate variations of a single mineral with intermediate structural or compositional characteristics (Hay, 1966).

Trace amounts of phillipsite were identified from Site 355 (Table 3) and were occasionally identified visually in some of the on-board coarse-fraction work, but phillipsite appears generally to be a minor constituent of South Atlantic sediments.

The three samples which are dominated by clinoptilolite (354-10, CC, 354-11-2, and 357-22-2) are

TABLE 3
X-Ray Powder Diffraction Data for Clinoptilolite

| 354-11-2, 99 cm | | Heulandite[a] | Clinoptilolite[a] |
|---|---|---|---|
| 2Θ | d (A°) | d (A°) | d (A°) |
| 9.842 | 8.987 | 8.90 | 9.00 |
| 11.292 | 7.836 | 7.94 | 7.94 |
| 13.093 | 6.762 | 6.80 | 6.77 |
| 17.244 | 5.142 | 5.09 | 5.11 |
| 19.144 | 4.636 | 4.69 | 4.69 |
| 22.495 | 3.952 | 3.97 | 3.96 |
| 24.145 | 3.685 | 3.71 | 3.73 |
| 25.045 | 3.555 | 3.56 | 3.55 |
| 26.045 | 3.421 | 3.40 | 3.42 |
| 26.596 | 3.351 | – | – |
| 28.246 | 3.159 | 3.12 | 3.12 |
| 28.796 | 3.100 | 3.07 | 3.07 |
| 30.096 | 2.969 | 2.97 | 2.97 |
| 32.047 | 2.793 | 2.80 | 2.80 |
| 32.947 | 2.718 | 2.72 | 2.72 |
| 35.397 | 2.536 | 2.48 | – |
| 37.148 | 2.420 | 2.43 | 2.42 |

[a]Selected lines from Mumpton (1960)

all from a carbonate-rich facies. These sites are located on topographically positive features (Site 354, Ceará Rise, Site 357, Rio Grande Rise) with a sediment section consisting predominantly of pelagic sediments with little terrestrial silt (Figures 1 and 4). The clay minerals in the Ceará Rise samples are mainly montmorillonite and kaolinite which are also common throughout the equatorial South Atlantic (Zimmerman, this volume). The Rio Grande Rise sample contains no clay minerals; the fine-grained material, as well as the silt fraction, is dominated by clinoptilolite.

Zeolite in the Brazil Basin (Site 355, Figure 4) is diluted by quartz and feldspar silts and montmorillonite clays. Some fine-grained clinoptilolite is also present, but only in trace amounts. Argentine Basin samples exhibit no zeolites in the silt-fraction in diffractograms, and only trace amounts of clinoptilolite with the clays, which are predominantly illite and montmorillonite. In this instance, zeolite was indicated by shipboard optical examination but not confirmed by X-ray diffraction (similarly, Sections 355-16-2, 356-17-3, 357-42-4, and 359-4-1). This result has also been noted by Berger and von Rad (1972), who suggest that zeolites must be rather abundant within the sediment in order to be identified through X-ray diffraction techniques. These samples were rechecked optically and in at least one case (359-4-1) euhedral zeolite laths were again commonly observed (Figure 3). The other samples also revealed trace amounts of clinoptilolite; their concentration apparently is below the detection limits of the X-ray methods used for this study (e.g., pretreatment with hydroxillamine may enhance the diffraction patterns).

## Distribution

Overall through the late Mesozoic and Cenozoic, we have 326 South Atlantic samples (each DSDP counted as one) of which 105 contain at least trace amounts of zeolites. This amounts to 32% of these samples, a surprisingly high number. Their distribution (Figure 5) shows a pronounced peak in the Paleocene, with approximately equal amounts during the Cretaceous, Eocene, Oligocene, and Miocene, and a decrease in the Pliocene. This variation is apparently not related to the number of sample positions per each epoch. Such a distribution substantiates observations by others that zeolite, in particular clinoptilolite, is most abundant in sediments of Miocene age or older (cf. Venkatarathnam and Biscaye, 1973). Zeolite distributions in surface sediments at the end of each epoch are illustrated in Figures 6-12.

### Cretaceous

Data points for the early Cretaceous (Figure 6) are very sparse, but the northerly area of zeolite occurrence is of significance inasmuch as it persists continuously through the Pliocene.

Coverage is considerably improved for the Late Cretaceous (Figure 7); zeolites seem to be concentrated along the topographic barrier formed by the ancestral Rio Grande Rise-Walvis Ridge and south of it. With the exception of the piston core sample within the bight formed by the Walvis Ridge and Africa, all samples along this barrier have volcanic glass shards associated with the zeolites. Two samples with zeolites from the continental margin of Argentina also contain volcanic material. A possible source for this volcanic detritus was volcanism on the central oceanic ridges, perhaps related to "hot-spot" activity (see discussion in McCoy and Zimmerman, this volume). Another possible source is the widespread Cretaceous volcanism in southern Brazil (Campos et al., 1974) which contributed volcanic components to sediments on the São Paulo Plateau. Related volcanism in the Salado Basin (Zambrano and Urien, 1970), just south of the modern Rio Plata estuary may also have contributed material to the Argentine continental margin and possibly to the northern Argentine Basin.

### Paleocene

Zeolite occurrences in the Paleocene (Figure 8) are similar to those of the Late Cretaceous. Volcanic materials were probably derived from the same sources.

Volcanic detritus in sediments of the São Paulo Plateau and large portions of the Brazil Basin is probably related to erosion of the extensive Cretaceous basalts in southern Brazil; Campos et al., (1974) also note that volcanism was active here during the Paleocene. Volcanic detritus in Argentine continental margin sediments could have been derived from Andean volcanism which was active during the Paleocene (Ruiz Fuller, quoted in Zambrano and Urien, 1970). Zambrano and Urien (1970) note that during the Paleocene the regional westward slope in Argentina changed to an eastward (Atlantic) slope. An influx of volcanic-rich sediments, therefore, may have occurred either through atmospheric transport of volcanic particles or through erosion of volcanic terrains by the newly established drainage patterns into the Atlantic.

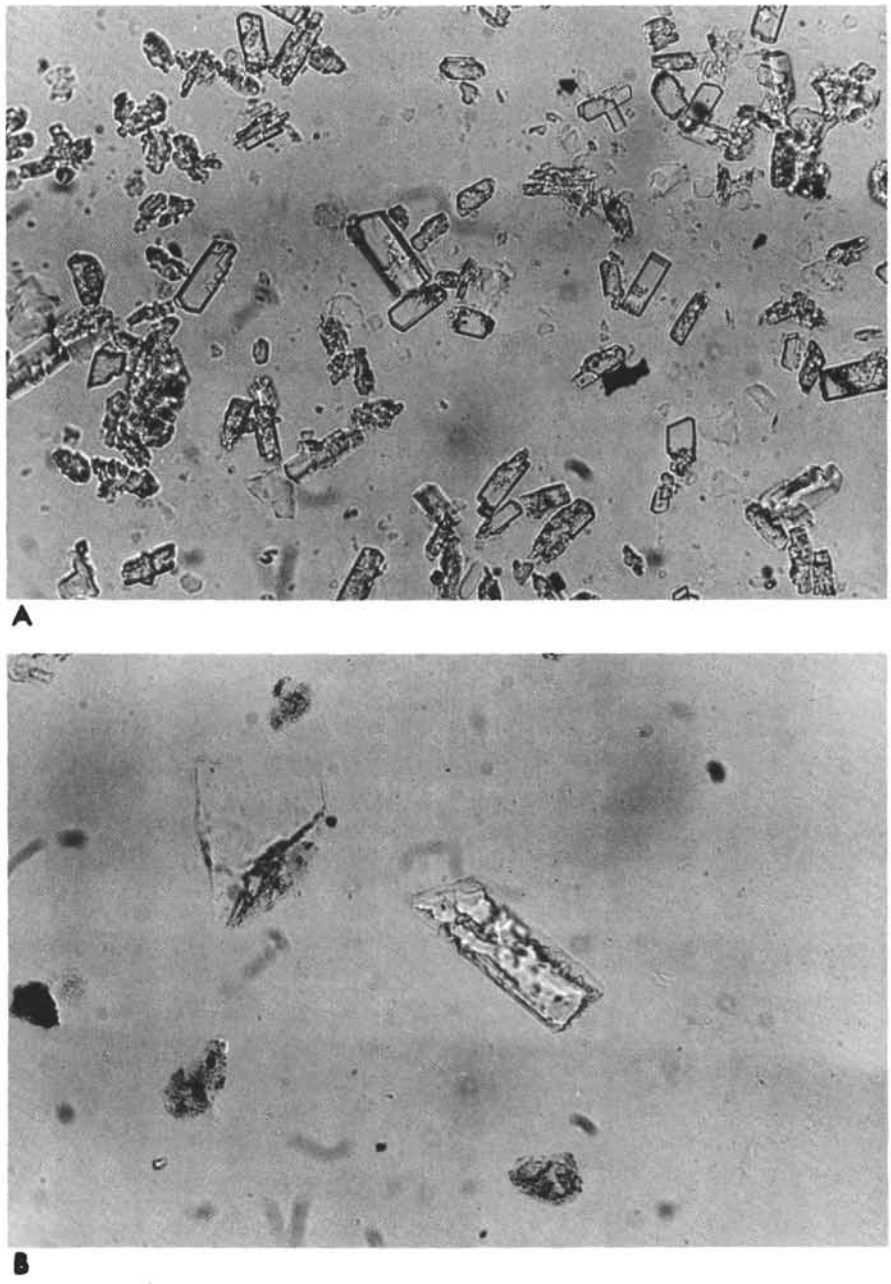

Figure 3. *Euhedral crystals of clinoptilolite (354-10 cc). 250×. Partial crystallization of zeolite on silicic core (359-4-1-139 cm). 250×.*

**Eocene**

Patterns in zeolite distribution at the end of the Eocene (Figure 9) remain somewhat similar to those described for the Cretaceous and Paleocene. Volcanic influence remains along the Mid-Atlantic Ridge and is inferred for the one sample in the equatorial area. On both the Walvis Ridge and Rio Grande Rise, volcanism is clearly indicated (Site Chapters 357 and 359, this volume). Presumably, volcanic material in the northern Argentine Basin (Site 358) and possibly along the Argentine continental margin may have been associated with erosion of volcanic terrains in South America and dispersal at sea by currents; the Argentine Basin could also be receiving this material from the north and east as well. Eocene volcanism took place just north of the São Paulo Plateau according to Campos et al., (1974) and would seem an additional source of volcanic material in the western South Atlantic.

On the São Paulo Plateau and Ceará Rise, Eocene zeolites are not associated with volcanic detritus, but with biosiliceous debris. Sediments from two piston cores on the Falkland Plateau are associated with biosiliceous lithofacies (McCoy and Zimmerman, this volume) as is partly the case at Site 355 (Brazil Basin) near a middle Eocene radiolarian clay. The bulk of the Eocene sediment cores in the Brazil Basin, however,

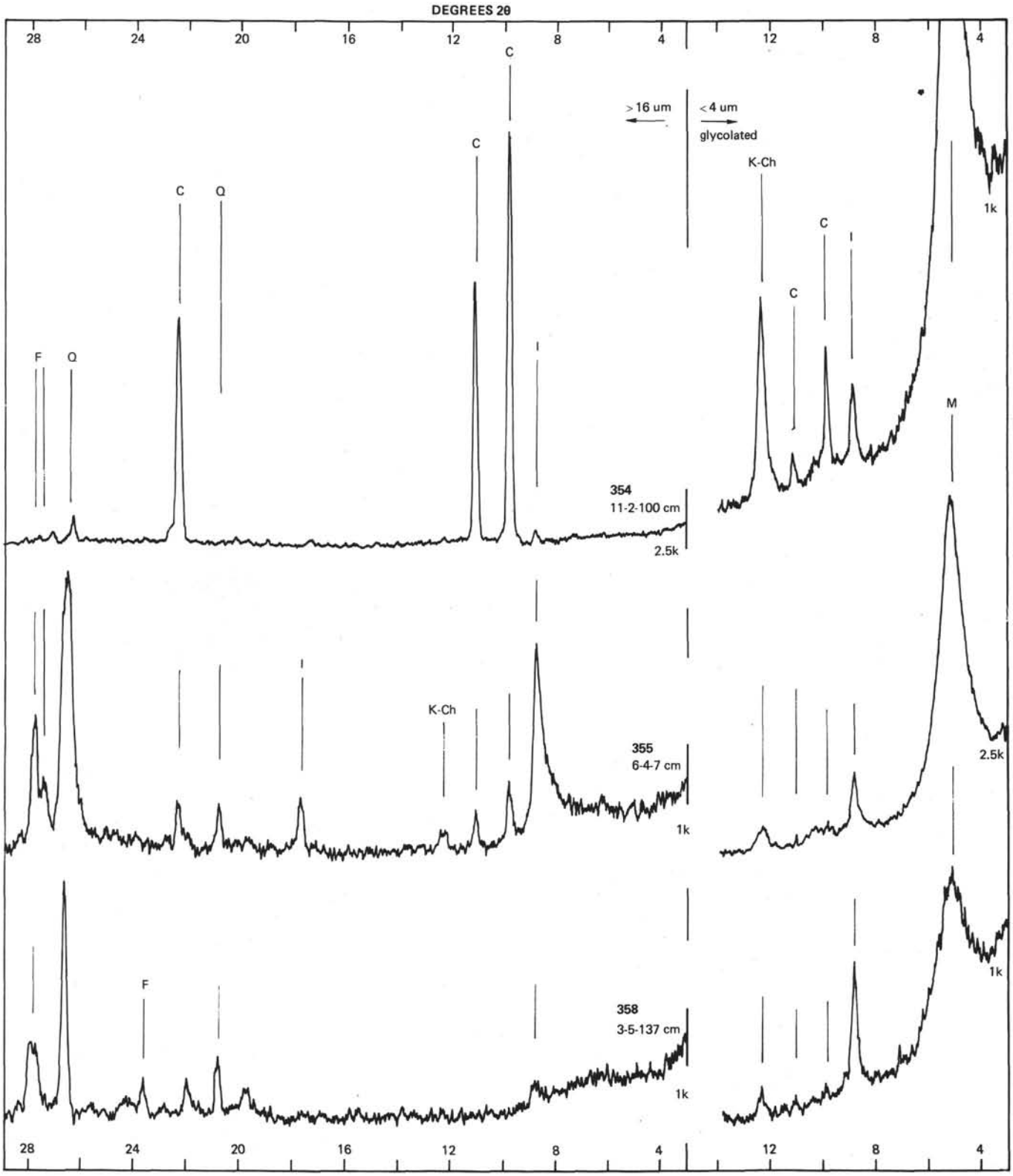


Figure 4. *Selected x-ray diffraction traces illustrating zeolite associations for South Atlantic sediments.*

represent a distal turbidite sequence containing numerous thin basal layers of quartz sand and silts within a clay matrix. These layers were apparently derived from the littoral zone based upon SEM studies on quartz grain surfaces of both sands and silts (Krinsley and McCoy, this volume). Zeolites were often found in these basal layers (Site Chapter 355, this volume) and SEM photographs show zeolites attached to quartz grains (Plate 1; compare with Mumpton and Ormsby, 1976). It may be that these more permeable

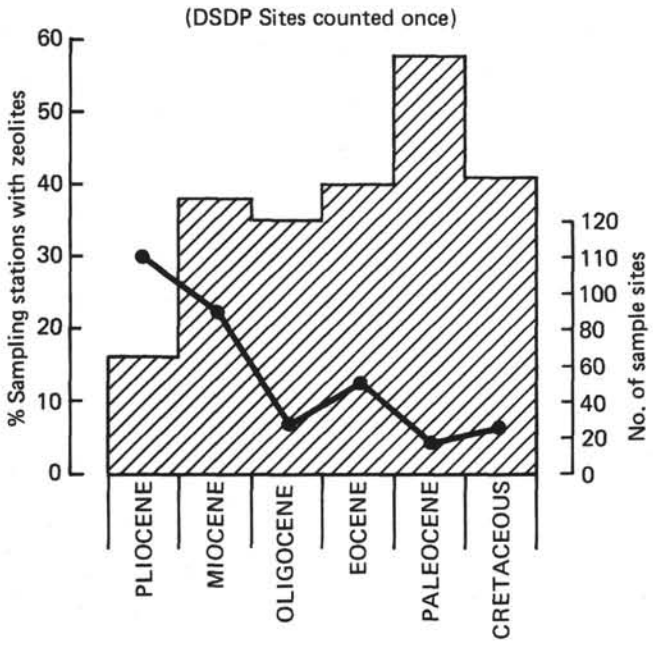


Figure 5. *Histogram portraying percent of sampling stations with sediments containing zeolites (trace amounts or more) as a function of geologic time. All sampling stations (piston cores, dredges, DSDP cores) counted as one point for each epoch to prevent a bias towards larger numbers of samples from thick sections drilled by DSDP (e.g., Eocene zeolitic muds at Site 355 in the Brazil Basin). With the exception of the Oligocene, the total number of samples from each time period that were available for study (solid line) do not influence the relative zeolite abundances through time. The high percentage of sampling sites containing zeolites in the Paleocene is particularly outstanding.*

sand and silt layers provided a conduit for the migration of pore water with the quartz grains acting as seed areas but not directly involved in the authigenesis. Quartz grains, in fact, show no indication of corrosion, instead they sometimes illustrate features more typical of chemical precipitation (see Plate 1).

### Oligocene

Data are poorer for the Oligocene (Figure 10) but the same general trends in zeolite distributions and host sediment associations continue. A very strong association of clinoptilolite with siliceous fossils is evident on the Ceará Rise. We suggest a larger area of zeolites in the Argentine Basin on the basis of preliminary data from Leg 39, probably reflecting increased biosiliceous activity related to the intrusion of Antarctic Bottom Water (AABW) which has increasingly influenced sediment types here since the Eocene (McCoy and Zimmerman, this volume).

### Miocene

With the distinctive increase in the number of samples (Figure 5), there is an apparent increase in the Miocene distribution of zeolites (Figure 11). These data illustrate the strong association of clinoptilolite with biosiliceous material in the Argentine and Cape basins where AABW intrusion, increased productivity of biosiliceous organisms, and complete dissolution of carbonates has carpeted these basins with biosiliceous clay (McCoy and Zimmerman, this volume). Zeolitic sediments also occur around Bouvet Island in the southern South Atlantic in part possibly reflecting volcanic material, and are still present in the equatorial area, but now also associated with biosiliceous material in both areas.

In the Brazil Basin, turbidites and clay continue to be associated with zeolites, the relationship being identical to that described here during the Eocene. The northerly extension of zeolite occurrences here may correspond to volcanism on Fernando de Noronha Island during the Miocene (Cordani, 1967, quoted in Gunn and Watkins, 1976).

Along the São Paulo Plateau and northern Brazilian continental margin, zeolite distributions delineate an area that has persisted since the Late Cretaceous. A volcanic association remains, although there is little evidence of extensive volcanism here during the Miocene; volcanism was at least locally active, however, as is well illustrated by the ash deposit on the São Paulo Plateau (see Site 356, this volume). The small patch of zeolites off northern Brazil lies directly off a small area of Miocene volcanism described by Campos et al., (1974). Volcanic detritus continues to be ubiquitous in association with zeolite sediments in the northern Argentine Basin (Site 358). The volcanic association along the central Mid-Atlantic Ridge, however, is largely inferred; no volcanic debris are identified in the smear slides.

### Pliocene

A distinct decrease in the areal distribution of zeolites occurs in sediments at the close of the Pliocene

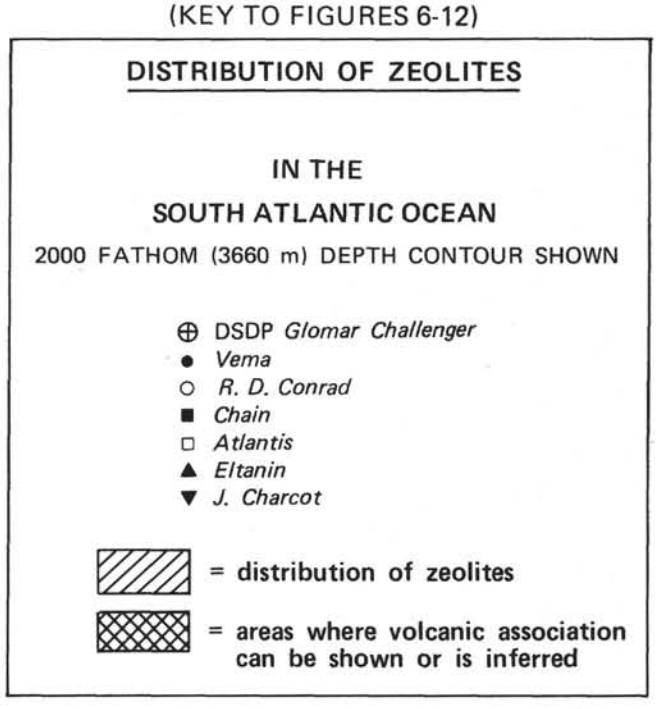

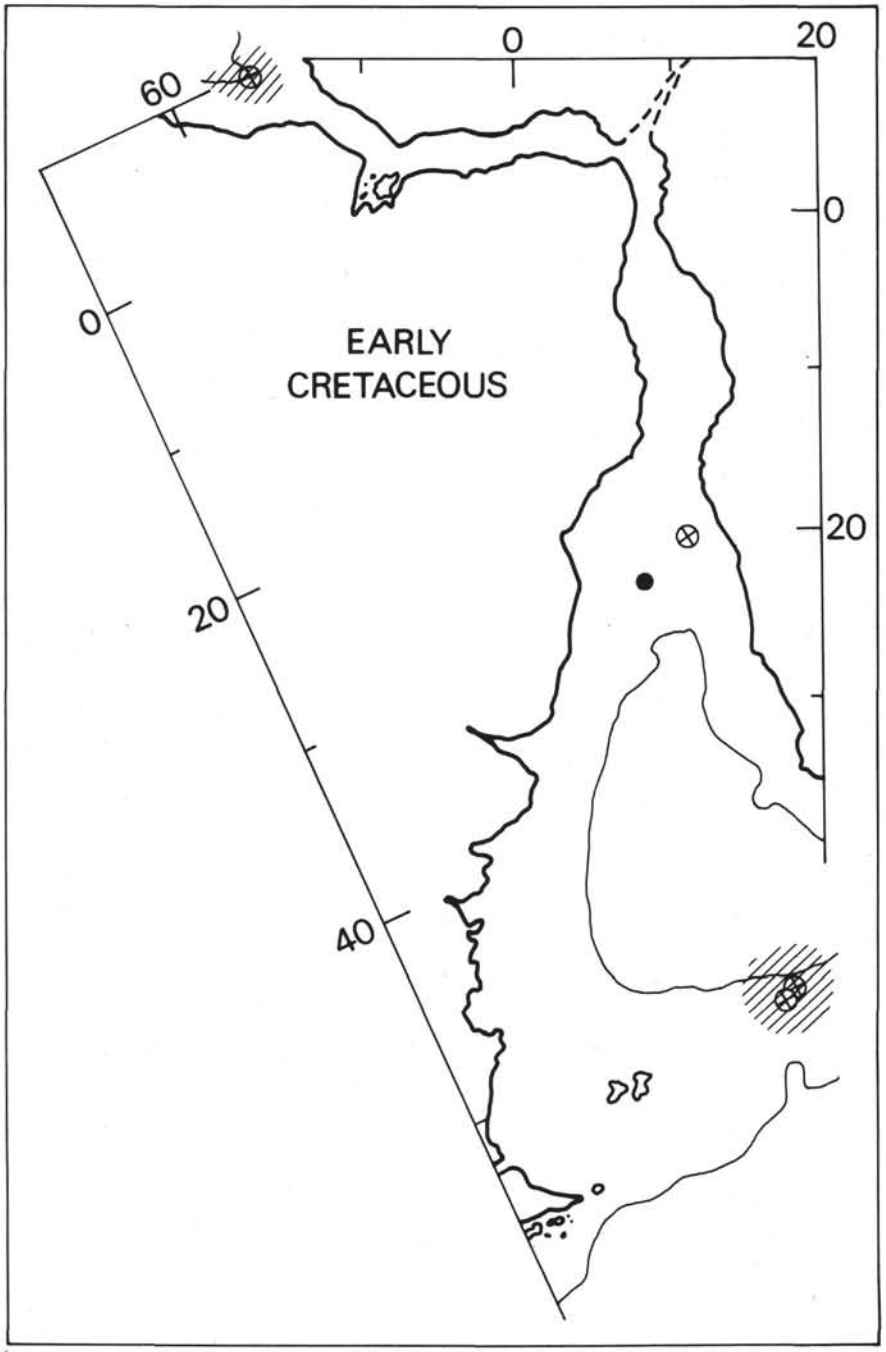


Figure 6. *Areal distribution of zeolites in sediments during the Early Cretaceous (pre-Albian). Hatchuring indicates approximate areal distribution of zeolitic sediments, cross-hatchuring indicates areas where volcanic association can be demonstrated or is inferred. Bathymetric contour is 200 fathoms (3660 m) based upon modern bathymetry and extrapolated back through each time period—this is only to show general physiographic outlines and is not meant to suggest paleobathymetry. See text for method of construction of palinspastic base maps. Modern coastal outlines shown for convenience.*

(Figure 12). A broad pattern still marks the Brazil Basin where turbidites continue to enter the basin. On the continental margin to the west, zeolitic sediments, often associated with volcanics, delineate a pattern somewhat similar to that noted for the Miocene.

Volcanic material and zeolites occur in an isolated patch east of the central Mid-Atlantic Ridge near St. Helena Island. According to Baker et al., (1967), volcanism was active here through the Pliocene. In equatorial areas, zeolites continue to be present in association with biosiliceous material.

Most surprising is the absence of zeolites in Argentine Basin sediments. Biosiliceous debris still forms the bulk of the sediment here during the Pliocene

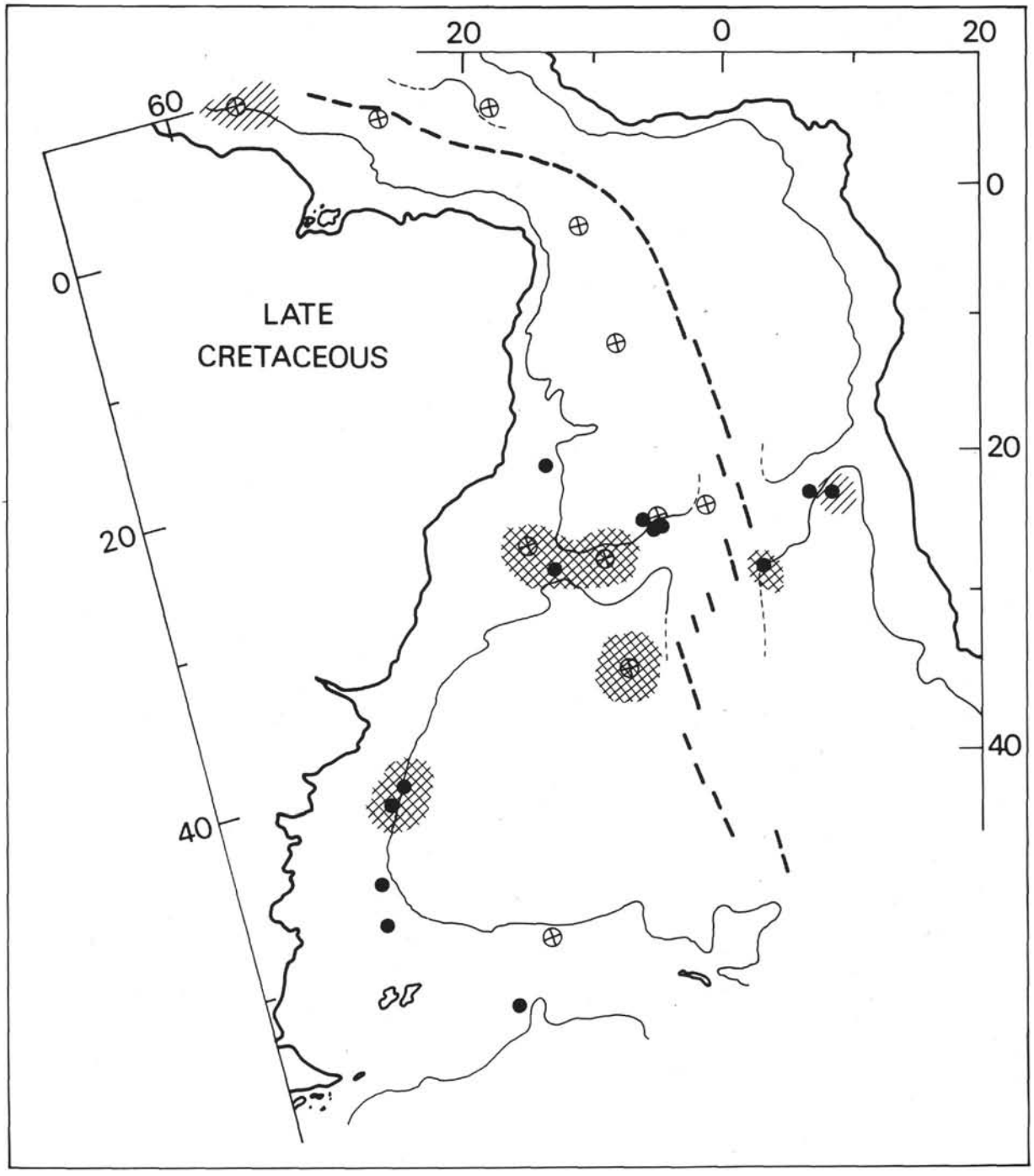


Figure 7. *Areal distribution of zeolites in sediments during the Late Cretaceous. Hatchuring indicates approximate areal distribution of zeolitic sediments, cross-hatchuring indicates areas where volcanic association can be demonstrated or is inferred. Bathymetric contour is 200 fathoms (3660 m) based upon modern bathymetry and extrapolated back through each time period–this is only to show general physiographic outlines and is not meant to suggest paleobathymetry. See text for method of construction of palinspastic base maps. Modern coastal outlines shown for convenience.*

(McCoy and Zimmerman, this volume). South of the Falkland Plateau, however, zeolites do occur. They are associated with volcanic material to the east; modern sediments just north of here in the Falkland Chasm are enriched in volcanic debris (Goodell, 1973; P. Ciesielski, personal communication). Zeolites continue to occur near Bouvet Island; volcanic material is present here in modern sediments (Goodell, 1973), but was not apparent in our Pliocene samples.

## DISCUSSION

Clinoptilolite occurs in association with three dominant sediment components; volcanic, biosiliceous, and turbidite/clays, each of which can provide a source

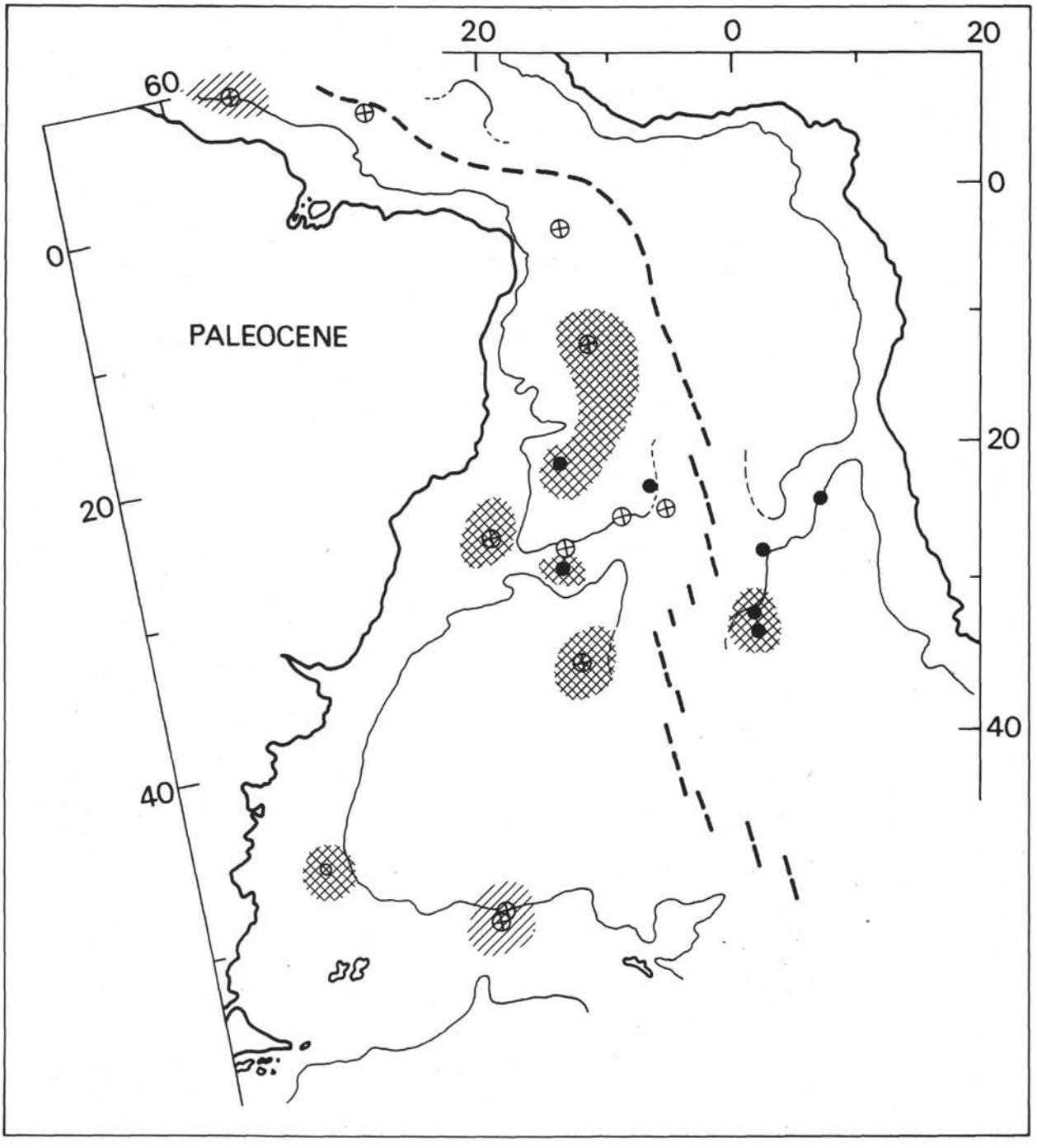


Figure 8. *Areal distribution of zeolites in sediments during the Paleocene. Hatchuring indicates approximate areal distribution of zeolitic sediments, cross-hatchuring indicates areas where volcanic association can be demonstrated or is inferred. Bathymetric contour is 200 fathoms (3660 m) based upon modern bathymetry and extrapolated back through each time period—this is only to show general physiographic outlines and is not meant to suggest paleobathymetry. See text for method of construction of palinspastic base maps. Modern coastal outlines shown for convenience.*

of silica for authigenic formation. These associations are somewhat loosely defined here, but the volcanic association appears to be dominant followed by the biosiliceous and terrigenous association (Figure 13). The formation of clinoptilolite may take place within a carbonate facies (e.g., Ceará Rise) under relatively high partial pressures of carbon dioxide (Zen and Thompson, 1974). One would expect that given the lower silica requirement for its formation and the ready availability of calcium, heulandite would form preferentially in the carbonate facies. However, we still observe clinoptilolite as the dominant zeolite. In these carbonate facies, biosiliceous material is also present and apparently required for the zeolite formation.

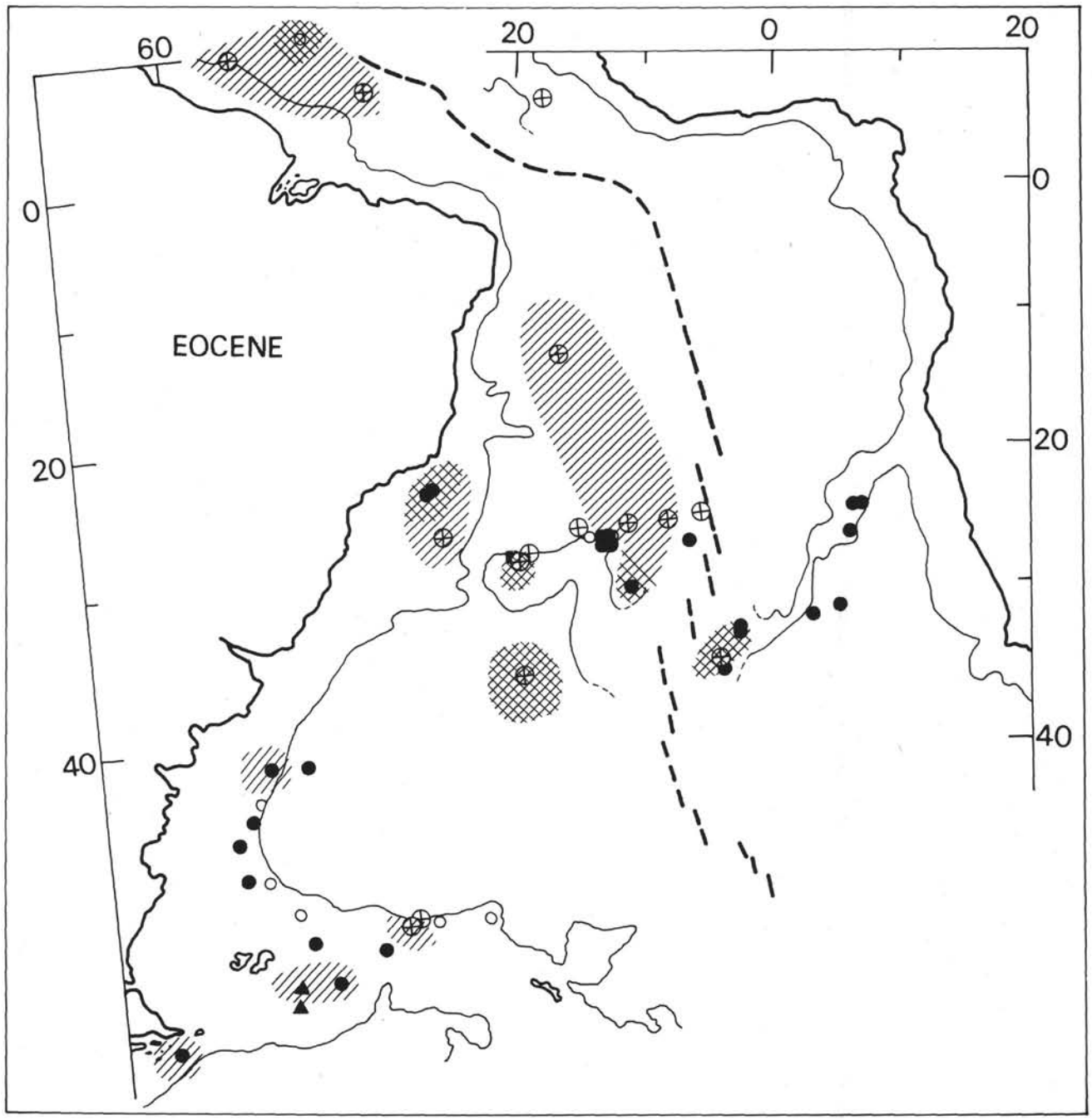


Figure 9. *Areal distribution of zeolites in sediments during the Eocene. Hatchuring indicates approximate areal distribution of zeolitic sediments, cross-hatchuring indicates areas where volcanic association can be demonstrated or is inferred. Bathymetric contour is 200 fathoms (3660 m) based upon modern bathymetry and extrapolated back through each time period–this is only to show general physiographic outlines and is not meant to suggest paleobathymetry. See text for method of construction of palinspastic base maps. Modern coastal outlines shown for convenience.*

Through time, the relative importance of these facies has changed significantly in South Atlantic deep-sea sediments (Figure 14) reflecting the development of lithofacies as the basin evolved (McCoy and Zimmerman, this volume). The volcanic association has decreased from 100% in the Cretaceous and Paleocene to 43% at the end of the Pliocene. Biosiliceous associations abruptly appear in the Eocene and remain at about constant levels through the rest of the Tertiary. The terrigenous association also becomes important in the late Tertiary, but generally seems to be the least influential. The formation of zeolite in these facies is apparently favored by the production of excess silica supplied by the devitrification of volcanic glass, dissolution of biosiliceous debris, or possibly through degradation of clays.

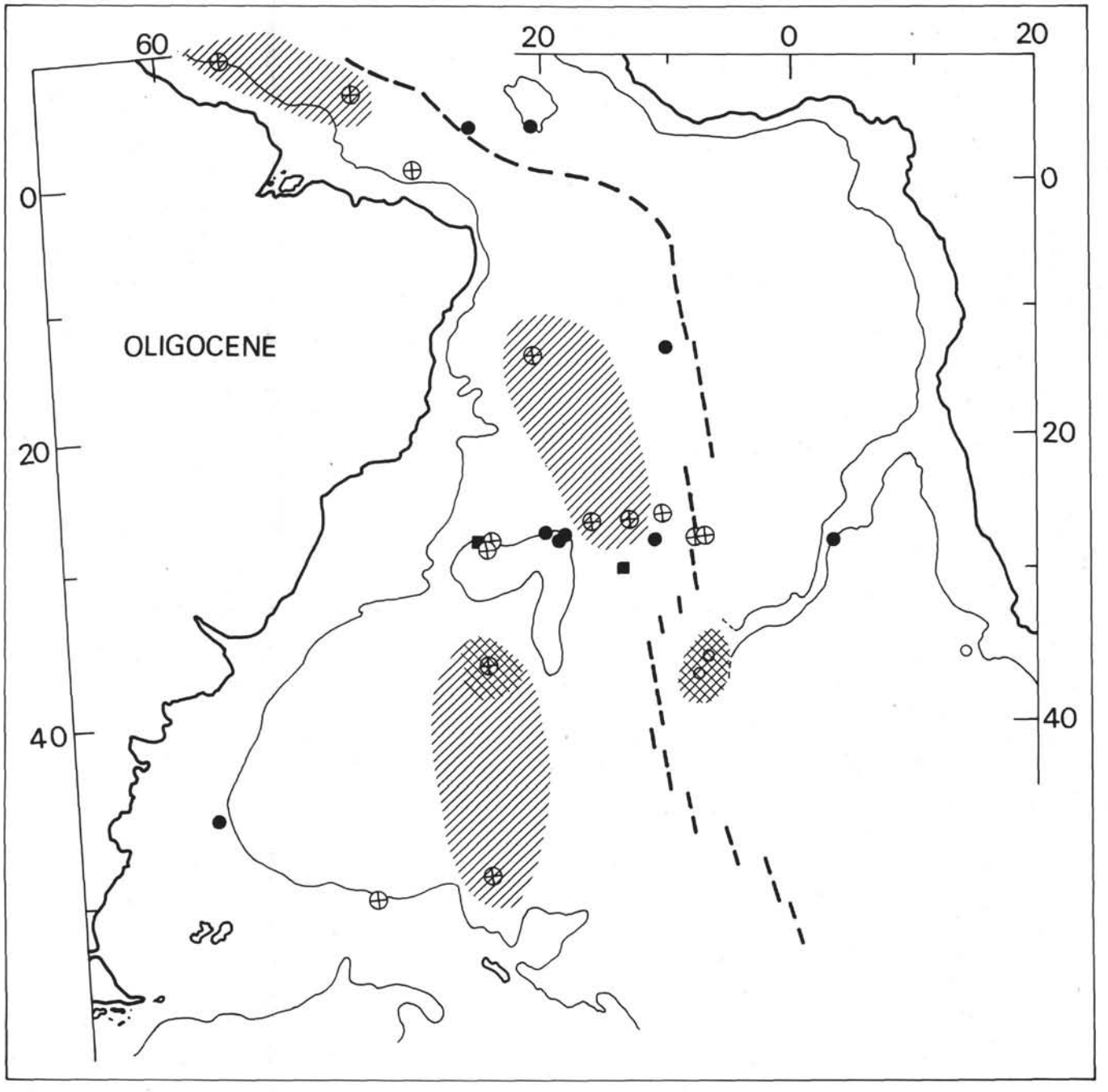


Figure 10. *Areal distribution of zeolites in sediments during the Oligocene. Hatchuring indicates approximate areal distribution of zeolitic sediments, cross-hatchuring indicates areas where volcanic association can be demonstrated or is inferred. Bathymetric contour is 200 fathoms (3660 m) based upon modern bathymetry and extrapolated back through each time period—this is only to show general physiographic outlines and is not meant to suggest paleobathymetry. See text for method of construction of palinspastic base maps. Modern coastal outlines shown for convenience.*

During the Cretaceous and Paleocene, the South Atlantic Ocean was a considerably smaller basin with the entire sea floor relatively close to continental sediment sources. Thus, any igneous activity on land or within the basin would be likely to distribute volcanic detritus over large portions of the sea floor. Apparently volcanic particles formed the precursor for the diagenetic development of zeolites during the early history of the South Atlantic. Siliceous biogenic activity at that time did not provide significant amounts of detritus to the deep-sea sediments (McCoy and Zimmerman, this volume). The advent of Antarctic glaciation and the formation of colder bottom waters which intruded into the Argentine and Cape basins led to the abrupt increase of biosiliceous components in the Eocene enabling this material to become an important source

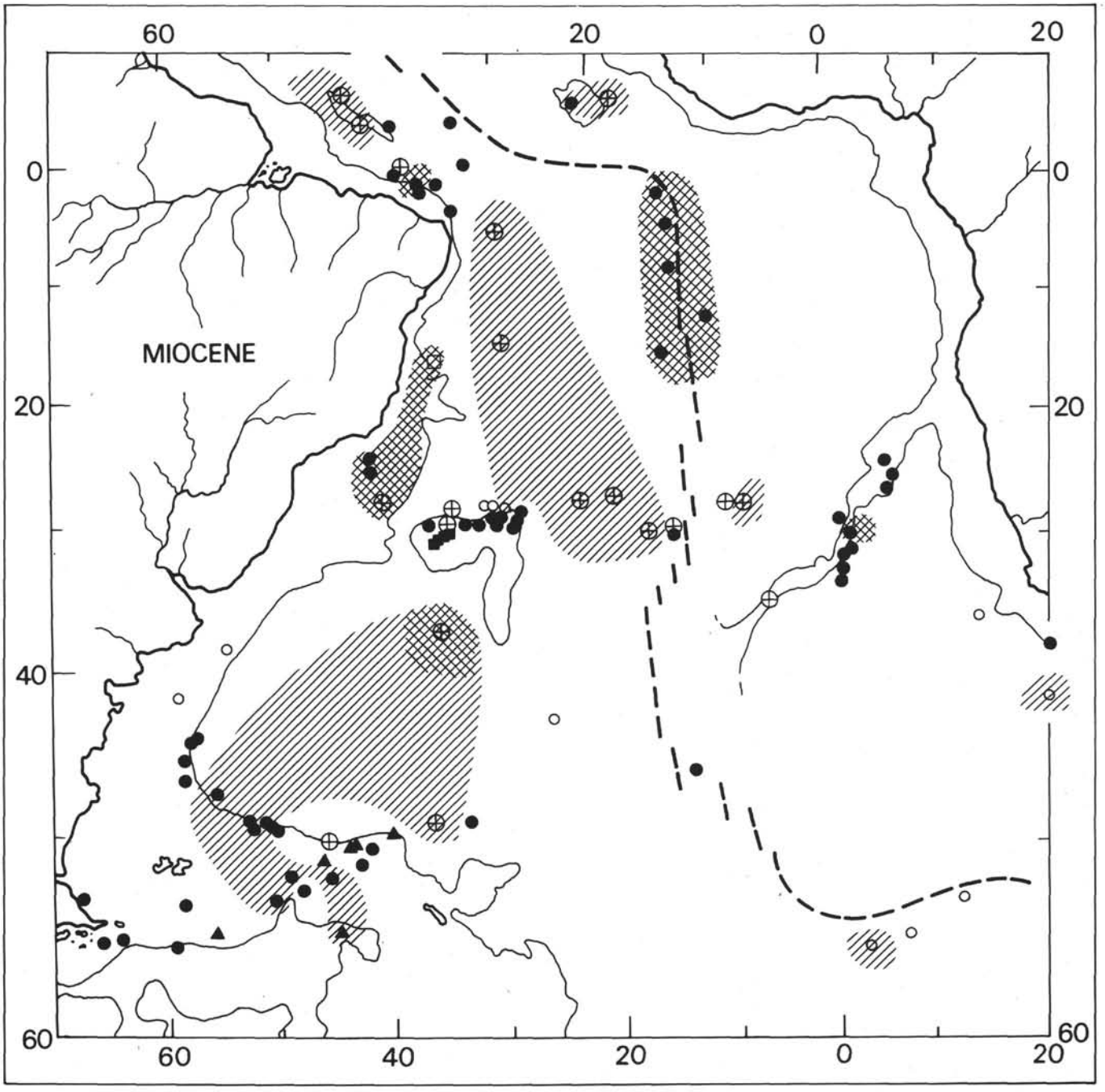


Figure 11. *Areal distribution of zeolites in sediments during the Miocene. Hatchuring indicates approximate areal distribution of zeolitic sediments, cross-hatchuring indicates areas where volcanic association can be demonstrated or is inferred. Bathymetric contour is 200 fathoms (3660 m) based upon modern bathymetry and extrapolated back through each time period—this is only to show general physiographic outlines and is not meant to suggest paleobathymetry. See text for method of construction of palinspastic maps. Modern coastal outlines shown for convenience.*

of excess silica. Both basins had also passed beneath CCD levels by the Eocene, carbonates were dissolved, and a clay-biosiliceous residue remained. Thus, both biosiliceous materials and clays may provide available precursors for zeolite formation in the post-Eocene.

The only strong authigenic association seems to be with well-crystallized clays of the montmorillonite group suggesting a common origin, probably from devitrification of volcanic glass (Peterson and Griffin, 1964). The persistence of montmorillonite, however, through the younger sediments in the absence of clinoptilolite, its generally common occurrence, and its absence at Section 357-22-2 where well-crystallized clinoptilolite is formed, suggest that this association is not critical to zeolite formation. Silt-sized, irregular masses of a silica were often seen in South Atlantic

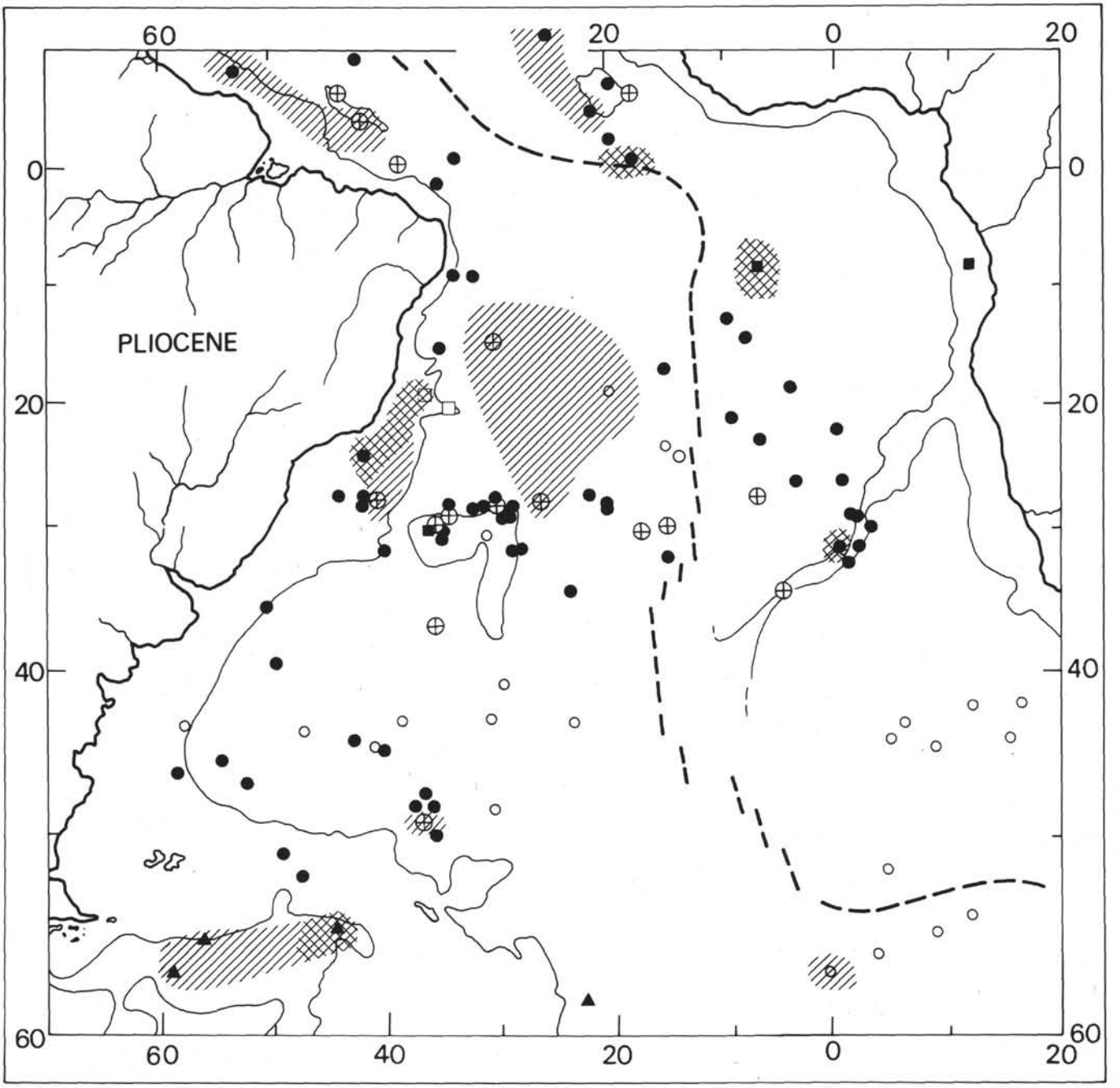


Figure 12. *Areal distribution of zeolites in sediments during the Pliocene. Hatchuring indicates approximate areal distribution of zeolitic sediments, cross-hatchuring indicates areas where volcanic association can be demonstrated or is inferred. Bathymetric contour is 200 fathoms (3660 m) based upon modern bathymetry and extrapolated back through each time period—this is only to show general physiographic outlines and is not meant to suggest paleobathymetry. See text for method of construction of palinspastic maps. Modern coastal outlines shown for convenience.*

sediments and tentatively identified as the partially dissolved remains of siliceous organisms. They may represent a transitional stage in the zeolite formation. Figure 3 illustrates this intermediate stage in the diagenetic process, with siliceous materials acting as a precipitation core and being partially altered to a euhedral zeolite crystal. (It is instructive to note that it was this sample that gave no X-ray trace for zeolite.)

It is interesting to note that the alteration of volcanic glass (and biosiliceous tests) is not a function of time; for instance, the bulk of the Cretaceous samples contains significant amounts of relatively unaltered and identifiable volcanic material. It is also notable that the rate of formation of zeolites may be indicated by the difference in Pliocene zeolite patterns (Figure 12) between the Argentine and Brazil basins. In the latter,

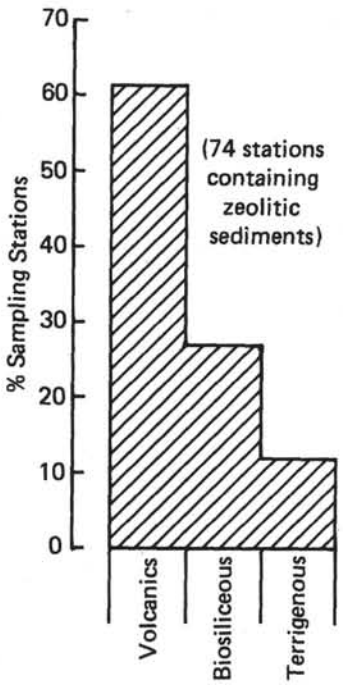


Figure 13. *Percent of sampling sites containing zeolitic sediments for all time periods in which a volcanic, biosiliceous, or terrigenous association can be demonstrated. See text for details. The dominance of a volcanic association is evident.*

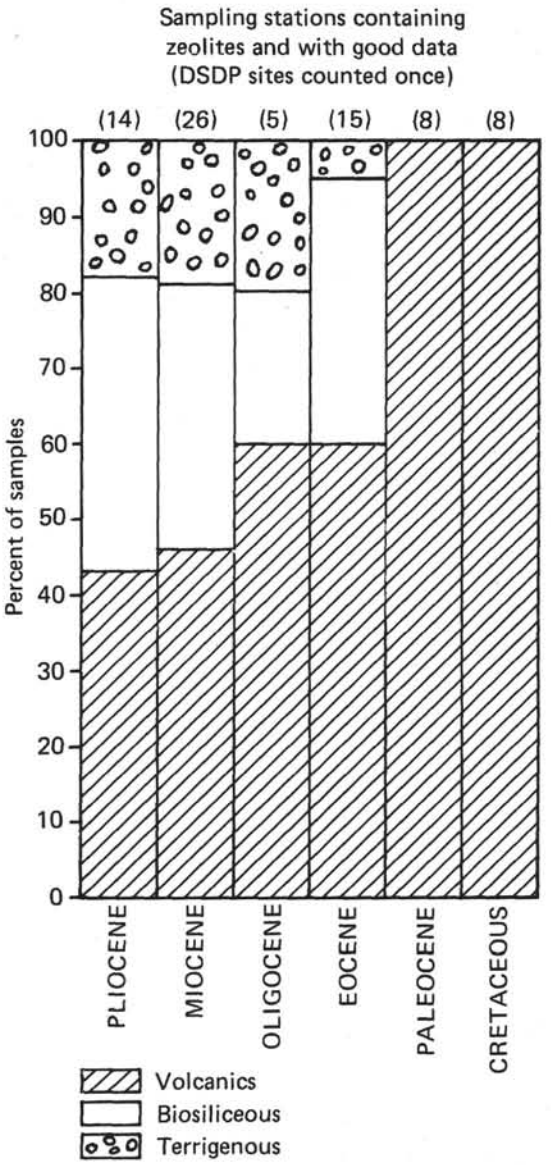


Figure 14. *Variation in zeolite sediment associations through time (DSDP sites counted as one sampling site for each epoch). Note the abrupt appearance of the biosiliceous and terrigenous associations from the Eocene onwards.*

zeolites occur over a broad area whereas they are apparently not common in the Pliocene sediments of the Argentine Basin. As noted previously, the presence of these thin but permeable sandy-silt layers of distal turbidite sequences in the Brazil Basin (Site 355) may permit more pore water migration, thereby allowing zeolites to form more quickly. Bonatti (1963) observed a similar occurrence in the Gulf of Alaska, an area of relatively high rates of silt deposition. The zeolite there, however, was phillipsite and the sediments were Recent in age.

In summary, the South Atlantic sediments show that clinoptilolite is commonly found associated with terrestrial, biosiliceous, and volcanic materials and that a high degree of diagenetic activity is evident in most deep-sea facies by the frequent occurrence of zeolite minerals.

## ACKNOWLEDGMENTS

We thank Mark D. Rogers for his aid with the powder diffraction analysis and Union College for use of the facilities of the X-ray Diffraction Laboratory. SEM work at Queens College was aided by the City University of New York Research Foundation. Support for the collection and curating facilities of the Lamont-Doherty Geological Observatory deep-sea sample collection is provided by the National Science Foundation through Grant No. OCE 76-18049 and the Office of Naval Research through Grant N00014-75-C-0210. We appreciate the assistance given by D. Cassidy for providing *Eltanin* samples from the Florida State University core repository, which is supported by Contract C-1059 from the National Science Foundation. Assistance by D. Johnson in providing *Chain* samples from the Woods Hole Oceanographic Institution core facility is also appreciated; this facility is supported by the National Science Foundation through Grant OCE 74-01744 and the Office of Naval Research through Grant N00014-74-C0262.

We appreciate the critical review and comments on this paper by E. Bonatti at L-DGO, B. Maynard at the University of Cincinnati, and M. Kastner at SIO.

## REFERENCES

Baker, I., Gale, N.H., and Simons, J., 1967. Geochronology of the St. Helena volcanoes: Nature, v. 215, p. 1451-1456.

Berger, W.H. and von Rad, U., 1972. Cretaceous and Cenozoic sediments from the Atlantic Ocean. *In* Hayes,

D.E., Pimm, A.C., et al., Initial Reports of the Deep Sea Drilling Project, Volume 14: Washington (U.S. Government Printing Office), p. 787.

Biscaye, P., 1965. Mineralogy and sedimentation of recent deep-sea clay in the Atlantic Ocean and adjacent seas and oceans: Geol. Soc. Am. Bull., v. 76, p. 803-832.

Bonatti, E., 1963. Zeolites in Pacific pelagic sediments: N.Y. Acad. Sci. Trans., v. 25, p. 938-948.

Campos, C.W.M., Ponte, F.C., and Miura, K., 1974. Goelogy of the Brazilian continental margin. *In* Burk, C.A. and Drake, C.L., (Eds), the geology of continental margins: p. 447-461.

Deer, W.A., Howie, R.A., and Zussman, J., 1963. Rock-forming minerals. v. 4: New York (John Wiley and Sons).

Goodell, H.G., 1973. Marine sediments of the southern oceans. *In* Goodell, H.G., et al., Marine sediments of the Southern Oceans, Antarctic Map Folio Series, Folio 17: Am. Geog. Soc.

Gunn, B.M. and Watkins, N.D., 1976. Geochemistry of the Cape Verde Islands and Fernando de Noronha: Geol. Soc. Am. Bul., v. 87, p. 1039-1100.

Hathaway, J.C. and Sachs, P.L., 1965. Sepiolite and clinoptilolite from the Mid-Atlantic Ridge: Am. Mineral., v. 50, p. 852-866.

Hay, R.L., 1966. Zeolites and zeolitic reactions in sedimentary rocks: Geol. Soc. Am. Spec. Paper, 85.

Jackson, M.L., 1969. Soil chemical analysis—advanced course: 2nd Ed., Pub. by the author, Dept. of Soil Science, University of Wisconsin, Madison.

Margolis, S., 1975. Paleoglacial history of Antarctica inferred from analysis of Leg 29 sediments by scanning electron microscopy. *In* Kennett, J.P., Houtz, R.E., et al., Initial Reports of the Deep Sea Drilling Project, Volume 29: Washington (U.S. Government Printing Office), p. 1039-1048.

Mehra, O.P. and Jackson, M.L., 1960. Iron oxide removal from soils and clays by a dithionate-citrate system buffered with sodium bicarbonate. *In* Swineford, A. (Ed.), Clays and Clay Minerals, 7th Nat. Conf. proc.: London (Pergamon Press).

Mumpton, F.A., 1960. Clinoptilolite redefined: Am. Mineral. v. 45, p. 351.

Mumpton, F.A. and Ormsby, W.C., 1976. Morphology of zeolites in sedimentary rocks by scanning electron microscopy: Clays and Clay Minerals, v. 24, p. 1-23.

Pitman, W.C., Larson, R.L., and Herron, E.M., 1974. The age of the ocean basins: Geol. Soc. Am., Map Series.

Peterson, M.N.A. and Griffin, J.J., 1964. Volcanism and clay minerals in the Southeastern Pacific: J. Mar. Res., v. 22, p. 13.

Rex, R.W., 1969. X-ray minerology studies—Leg 1; *In* Ewing, M., Worzel, J.L., et al., Initial Reports of the Deep Sea Drilling Project, Volume 1: Washington (U.S. Government Printing Office), p. 354.

Saito, T., Burkle, L.H., and Hays, J.D., 1974. Implications of some pre-Quaternary sediment cores and dredges. *In* Hay, W.W. (Ed), Studies in Paleo-oceanography: Soc. Econ. Paleont. Mineral. Spec. Publ. No. 20, p. 6-36.

Venkatarathnam, K. and Biscaye, P., 1973. Deep-sea zeolites: variations in space and time in the sediments of the Indian Ocean: Mar. Geol., v. 15, p. M11-M17.

Zambrano, J.J. and Urien, C.M., 1970. Geological outline of the basins in southern Argentina and their continuation off the Atlantic shore: J. Geophys. Res., v. 75, p. 1363-1396.

Zemmels, I. and Cook, H.E., 1973. X-ray mineralogy of sediments from the central Pacific Ocean. *In* Winterer, E.L., Ewing, J.I., et al., Initial Reports of the Deep Sea Drilling Project, Volume 15: Washington (U.S. Government Printing Office), p. 517.

Zen, E-An, and Thompson, A.B., 1974. Low grade regional metamorphism: mineral equilibrium relations. *In* Donath, F.A. et al. (Eds.), Ann. Rev. Earth Planet. Sci., v. 2: Palo Alto Annual Reviews Inc., p. 179.

## PLATE 1

Figure 1 — Zeolites clustered in depression on quartz sand grain which has been subjected to subaqueous action. Note mechanical "V"-shaped patterns on raised areas. 1 $\mu$m = 1 mm.

Figure 2 — Zeolites growing on quartz sand surface. Note that there appears to have been some silica precipitation after the zeolites formed. Also note that the original (?) grain surface appears to have been subjected to precipitation; it is quite smooth. 1 $\mu$m = 1 mm.

Figure 3 — Zeolites on quartz grain surface; the surface itself is the result of conchoidal breakage. 1 $\mu$m = 1 mm.

Figure 4 — Quartz grain surface with probable zeolite in hollow. Surrounding the hollow, on the high areas, are mechanical "v's," indicating subaqueous littoral and/or shelf abrasion. 1 $\mu$m = 1 mm.

Figure 5 — Partially rounded quartz sand grain with zeolites scattered across surface. 1 $\mu$m = .25 mm.

Figure 6 — Irregular quartz sand grain with zeolites scattered across surfaces. The grain was probably abraded in the littoral or shelf zone; note the fresh, mechanical "V"-shaped patterns. 1 $\mu$m = .2 mm.

Figure 7 — Probable zeolites on surface of quartz sand grain. Note mechanical "V"-shaped patterns indicating littoral action. Some etching can also be seen; note large "V"-shaped patterns en echelon. 1 $\mu$m = 3.5 mm.

Figure 8 — Irregular precipitation and etch surface on quartz sand grain with a few zeolites scattered across the surface. 1 $\mu$m = 1 mm.

Figure 9 — Irregular quartz sand grain with zeolites scattered across the surface. The fiber to the right of the grain is the result of contamination. 1 $\mu$m = .16 mm.

Figure 10 — Zeolites on quartz sand surface. Note the silica precipitation following zeolite growth; the zeolites appear to be cemented to the grain surface by silica. 1 $\mu$m = 1 mm.

Figure 11 — Zeolites resting on conchoidal quartz sand surface. 1 $\mu$m = 3.6 mm.

Figure 12 — Several zeolites on quartz sand surface. Note "V"-shaped patterns which represent littoral and/or shelf abrasion. 1 $\mu$m = 3.6 mm.

## PLATE 1

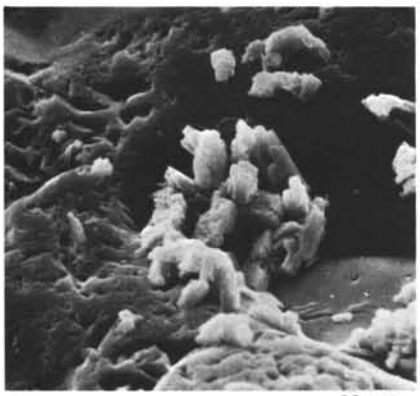
1 20 μm

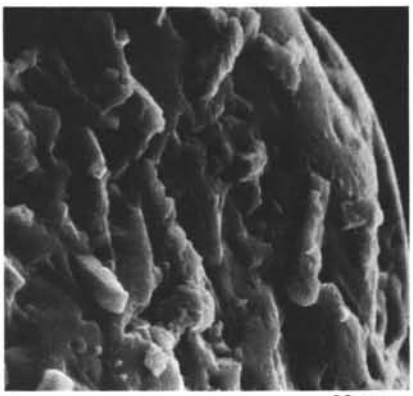
2 20 μm

3 20 μm

4 20 μm

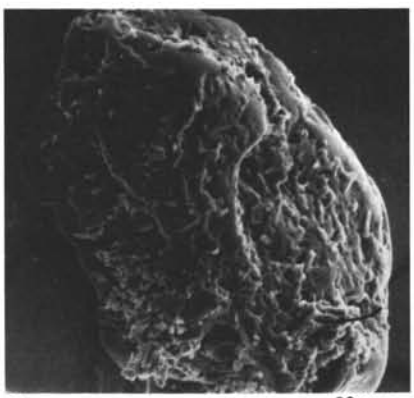
5 80 μm

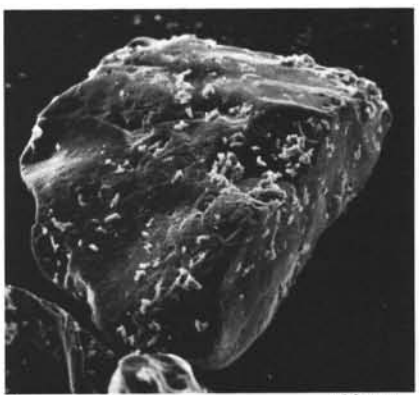
6 100 μm

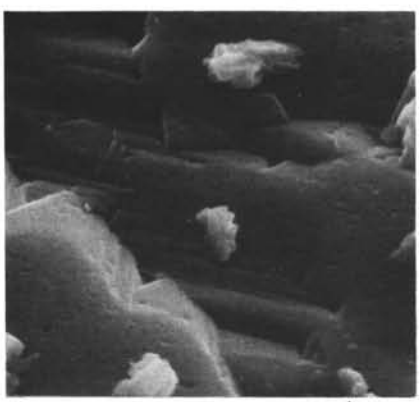
7 6 μm

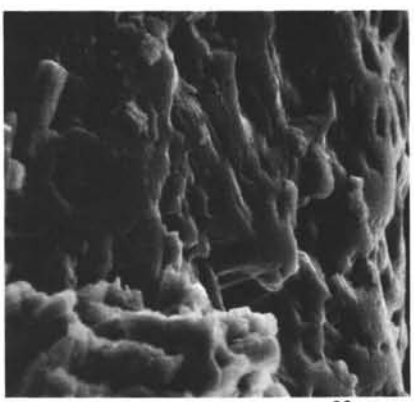
8 20 μm

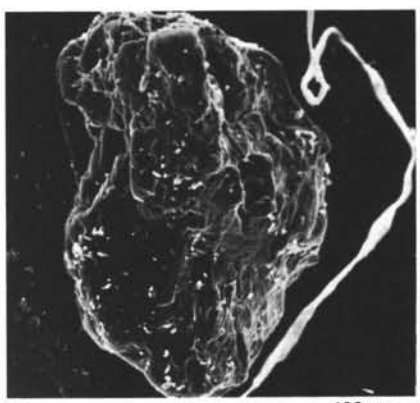
9 130 μm

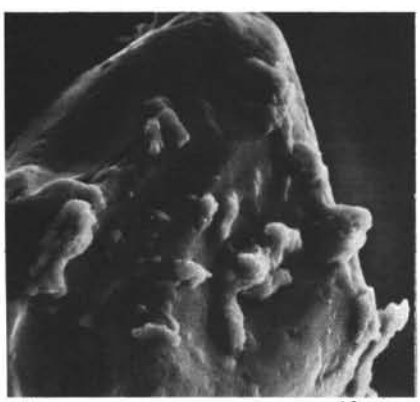
10 20 μm

11 6 μm

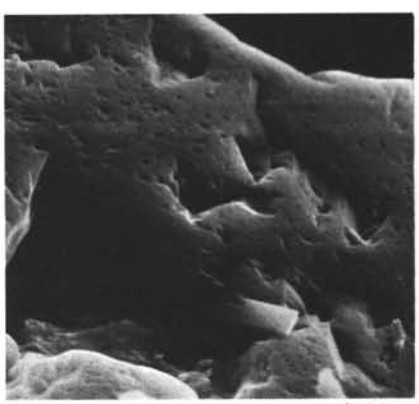
12 6 μm